Original Article

Cite This: Colloid & Nanoscience Journal 1 (2023) 83-96.

CNJ.araku.ac.ir

Co-deposition of COOH-POSS on the surface of PES nanofiltration membranes for improving the permeability and anti-fouling properties

Zahra Safikhani[1], Abdolreza Moghadassi[1*], Samaneh Bandehali[*1], Farideh Ahmadi[1], Maryam Ghafari[1]

Received:2023-01-31
Revised: 2023-05-24
Accepted: 2023-05-24
DOI: **10.52547/CNJ.1.2.83**

[1] Department of Chemical Engineering, Arak university, Arak 38156-8-8349, Iran

Abstract

In this study, a new type of polyethersulfone (PES)-based nanofiltration (NF) membrane was fabricated through the modification of membranes surface by using 4-aminobutyric acid-functionalized glycidyl POSS for the improvement of the physicochemical properties and membrane separation performance. Scanning electron microscopy (SEM), Fourier transform infrared spectroscopy (FTIR), and 3D surface images, pure water flux, water content, water contact angle, salt rejection were used in membrane characterization. The SEM images showed the finger like structure for the modified membranes. Moreover, the SEM images of the membrane surface revealed the excellent dispersion of modified POSS particles on the membrane surface. The water content angle of fabricated membranes declined compared to the virgin PES membrane that indicates the enhancement of membrane hydrophilicity. Water content of the fabricated membranes enhanced from 68% for the neat PES membrane to 77.55% for the one fabricated membrane. However, the pure water flux revealed the decline trend. But among prepared membranes, M3 at 1.5 wt.% COOH-POSS concentration showed the best $CrSO_4$ rejection (80%) and Na_2SO_4 rejection (62%). Moreover, M1 at 0.5 wt.% of COO-POSS showed the $Pb(NO_3)_2$ and $Cu(NO_3)_2$ rejection 83% and 80%, respectively.

Keywords: Polyethersulfone, Nanofiltration membranes, 4-aminobutyric acid, Octaglycidyloxypropyl-silsesquioxane, Salt removal

1. Introduction

These days, increasing demand for freshwater is the most important reason for the improvement of membrane technologies for the wastewater revival and desalination [1-4]. Nanofiltration (NF) membrane has high rejection for multivalent ions [5, 6]. High removal of pollutants, passable chemical and mechanical resistance, improvement of antifouling properties and long-life are considered as the main properties in the knowledge of membrane [7, 8]. Membrane surface modification such as grafting, surface coating and other different treatments such as UV irradiation, plasma treatment, and chemical treatment is a promising technique to the increment of the membrane separation properties. Meanwhile, introducing inorganic nanoscale materials on the surface of membrane is the routes to improve membrane separation performance [9-14]. Different nanomaterials were studied such as metal oxide nanoparticles, graphene oxide (GO) nanosheets, carbon nanotubes (CNT), metal-organic frameworks (MOFs) and etc [15-18].

Xiong et al. [19] fabricated PES-based NF membranes from polyethylenimine (PEI), glutaraldehyde (GA) and carboxymethyl chitosan (NO-CMC) by layer-by-layer method. The antibiological fouling performance of the fabricated membranes improved by coating silver nanoparticles (AgNPs) on the membrane surface. The results exhibited the rejection of salt in the order of $MgCl_2$ > $MgSO_4$ > $CaCl_2$ >Na_2CO_3 > NaCl > Na_2SO_4. Moreover, the fabricated membranes revealed the rejection of heavy metals for Cr^{3+}:88.95%, Cu^{2+}:84.04%, Cd^{2+}: 82.69% and Ni^{2+}: 83.47%. Huang et al. [20] used Ag@ZnO-Oleic acid (OAc) core-shell nanoparticles for the fabrication of polyamide (PA) thin-film nanocomposite (TFN) membranes by trimesoyl chloride (TMC) solutions in an interfacial polymerization process. The physicochemical properties of TFN membranes improved by applying nanoparticles. These membranes showed higher salt rejection and a lower decline of flux in BSA filtration compared with the TFC membrane without nanoparticle. Li et al. [21] applied a facile mussel-inspired method for the preparation of loose nanofiltration membranes. The deposition of polydopamine (PDA) on the membrane surface was performed by hydroxyl radical activation generated by $CuSO_4/H_2O_2$. Moreover, a zwitterionic polymer (SBMA) used for PDA/SBMA co-deposition via polymerization. The application of SBMA led to an

Corresponding Authors:
zeo.sercher@yahoo.com

electroneutral, anti-fouling and anti-bacterial surface properties. The optimum property such as anti-fouling performance and dye rejection was revealed for 2 mg/mL PDA and 2 mg/mL SBMA.
Shen et al. [22] reported the grafting poly(methyl methacrylate) with multi-walled carbon nanotubes (MWNTs) and the functionalization of carbon nanotube (CNT) for the fabrication of TFN PA membranes. These membranes showed high Na_2SO_4 rejection (99%) with an increase of 62% in pure water flux. Vatanpour and Khorshidi [23] reported the surface modification of porous polyvinylidene fluoride (PVDF) membranes by a layer of ultra-thin zeolitic imidazolate framework-8 (ZIF-8). The ZIF-8 layer was produced from the reaction between Zn^{2+} aqueous solution and 2-methylimidazole/n-hexane solution and immersing PVDF membranes. As stated in the results hydrophilicity and pure water flux of membranes has improved significantly. Moreover, membranes showed high antifouling properties.

Polyhedral oligosilsesquioxane (POSS) is determined as a nanoparticle that includes silica cage nucleus and top groups. The chemical formula of POSS is $(RSiO1.5)n$ R is top groups, such as aryl , alkene, hydrogen, alkyl, halogen [24]. Good dispersity and adaptability with polymers are good features for POSS. Several studies have been done about treatment of waste water by modification of surface membrane that has been used POSS as nanoparticle. Koutahzadeh et al. [25] fabricated POSS into the polysulfone (PSf) matrix in ultrafiltration membranes. The modified membranes indicated higher hydrophilicity compared to the neat membranes in this study. The permeability of the fabricated membranes increased from 33 for to 215.2 M-2h-1 for the bare PSf membrane and POSS-PSf with 2 wt.% of POSS, respectively. The flux recovery ratio was enhanced from 50.6% for the pure PSf membrane to 75% and 62% for POSS-PSf at 0.5% and 1wt.% POSS, respectively. Also, the best results, such as suitable antifouling properties and good permeability were gained for 0.5wt% of POSS. Sun et al. [26] fabricated polyvinylidene fluoride (PVDF)/EG-POSS. EG-POSS is the grafting between ethylene glycol (EG) and POSS. Conforming to the results antifouling properties and hydrophilicity of membranes increased by using EG-POSS. You et al. [27] modified the polyamide membrane by functionalization of POSS by polyethylene glycol. The charge and hydrophilicity of the membrane surface improved in comparison to the neat membrane. The highest pure water flux measured 38.7 Lm^2h^{-1} at 0.2MPa without reducing the Na_2So_4 rejection (87.1-91.6%). He et al. [28] prepared POSS-polyamide membranes by interfacial polymerization. The membranes were used to the separation of selenium and arsenic. The highest rejection of SeO_3^{2-}, SeO_4^{2-} and $HASeO_4^{2-}$ was obtained 93.9, 96.5 and 97.4% for TFN membrane containing 0.15 wt.% UiO-66, respectively.

In this work, the phase inversion technique was employed to fabricate the polyethersulfone (PES) NF membranes. PES membrane is inherently hydrophobic that affects membrane fouling. The improvement of antifouling abilities and surface hydrophilicity of nanofiltration membranes can be achieved by applying graft polymerization, surface coating and the incorporation of inorganic nanofillers [29, 30].
Herein, 4-aminobutyric acid was employed to the functionalization of glycidyl-POSS. Carboxyl and amine groups in 4-aminobutyric acid improved membrane surface hydophilicity and compatibility. Then the membranes were fabricated by coating functional glycidyl POSS (COOH-POSS) on the PES membrane surface. FTIR, SEM, 3D surface images, water content and contact angle were applied to characterize the fabricated membranes. The effect of different concentrations of COOH-POSS was studied on the physicochemical properties, membrane morphology, antifouling properties and separation performance. The ability of COOH-POSS/PES membrane in the separation of Na_2SO_4, $Cr(SO_4)_2$, $Cu(NO_3)_2$ and $Pb(NO_3)_2$ from the water was studied.

2. Materials and methods

2.1. Materials

Polyethersulfone (PES) (M_W=58,000 g/mol) as the membrane matrix was supplied by BASF company New Jersey, USA (Ultrason E6020P, M_W:58,000, T_g:225 °C). The N,N dimethylacetamide (DMAC: 87.12 g/mol, 0.94 g/cm^3) was obtained from DAEJUNG, Korea. Octaglycidyloxypropyl-silsesquioxane (glycidyl POSS) was provided from Iran Polymer and Petrochemical Institute. The polyvinylpyrrolidone (PVP: 25,000 g/mol) was purchased from Merck, Inc., Germany. Glutaraldehyde (GA) aqueous solution (Grade II, 25%) was supplied from Sigma-Aldrich. 4-aminobutyric acid was purchased from Sigma-Aldrich. Na_2SO_4, $Pb(NO_3)_2$, $Cr(SO_4)_2$ and $Cu(NO_3)_2$ salts were supplied by Merck, Inc., Germany and applied to prepare feed solutions for the membrane separation studies.

2.2. Fabrication of PES membrane

PES membranes were fabricated via phase inversion technique and immersion into the water bath. PES (18 wt.%) and PVP (1 wt.%) were dissolved in DMAC. After stirring solution for 5 h to achieve homogeneous solution, the prepared solution was left at room temperature for one day for removal of dissolved air bubbles. Then an applicator was used to cast the prepared solution on the dry and clean glass plate, and then immersed in a bath of deionized water for one day. After that membranes were dried between paper sheets for 24 h at the room temperature.
For surface modification of PES membrane, the different ratio of POSS and 4-aminobutyric acid (0, 0.5, 1 and 1.5 wt.%) was added to the aqueous solution and was stirred for 2h at 50 °C. Then the prepared solution was

sonicated by Ultrasonic instrument (Parsonic 11S model, S/N PN-88159, Iran) for 1 h. The PES membranes were put on the clean and dry glass plates then the prepared solution was poured on the surface of membranes. After 5 min the membranes were put in an oven for 3h at 50 °C. Fig. 1 exhibited the chemical structure of 4-aminobutyric acid functionalized POSS (COOH-POSS).

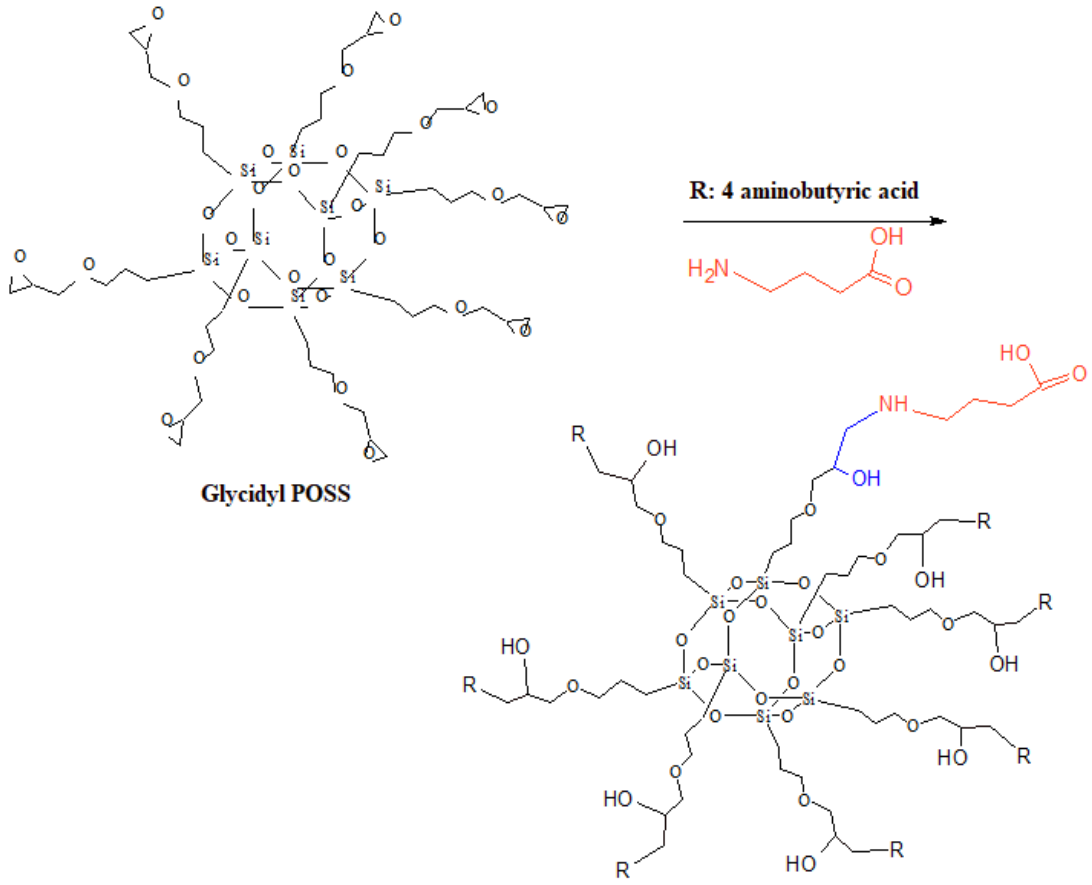

Fig. 1. Schematic diagram of 4-aminobutyric acid functionalized POSS (COOH-POSS).

2.3. Characterization of membrane

The membranes morphology was explored by SEM images. Before analysis, the membrane samples were kept in the liquid nitrogen and then were broken. The gold was employed to sputter the sample of membranes for providing electrical conductivity.

The measurements of water contact angle (θ) of the fabricated membranes were performed by contact angle analyzer (G10, Kruss, Germany) and used to study the hydrophilicity of the membrane surface via deionized water as probe liquid.

The membrane porosity (ε) was evaluated by the below equation:

$$\varepsilon(\%) = \left(\frac{W_w - W_d}{\rho_f V_m}\right) \times 100 \quad (1)$$

Where W_d and W_w are the weight of dry and wet membrane (g). V_m and ρ_f are membrane volume (cm^3) and water density (g/cm^3), respectively. For decreasing test errors, all the experiments were performed three times and then their averages were computed.

The mean pore sizes of produced membranes were measured by Guerout–Elford–Ferry equation (2) [31]:

$$r_m = \sqrt{\frac{(2.9 - 1.75\varepsilon)8\eta LQ}{\varepsilon A \Delta p}} \quad (2)$$

Where η is the viscosity of water (8.9×10^{-4} Pa.s), Q and ΔP are the volume of the permeated pure water flux (m^3/s), and operating pressure (0.45 MPa), ε, A and L are the membrane porosity, the membrane filtration area (m^2) and the membrane thickness (m).

2.4. Membrane filtration performance

The salt rejection and pure water flux for the fabricated membrane was evaluated by cross-flow NF system. The prepared membranes were compacted with distilled water for 1 h at 4.5 bar to gain steady state conditions. Then filtration test was done at 4.5 bar and 25°C. The permeation flux was computed by the equation (3):

$$J_{w,1} = \frac{V}{A \times t} \quad (3)$$

Where $J_{w,1}$ is the permeate flux ($Lm^{-2}h^{-1}$), A is the membrane surface area (11.94 cm^2), t is the filtration time (h) and V is the volume of collected permeate (L).

The membrane rejection was determined by equation (4):

$$R(\%) = \left(1 - \frac{C_p}{C_f}\right) \times 100 \quad (4)$$

Where C_f and C_p are the concentration of feed solution and permeate, respectively.

All filtration performance was done three times to reduce experimental errors.

The antifouling properties of the fabricated membranes were investigated by the flux recovery ratio (FRR). Milk powder solution was used to evaluate antifouling performance of the prepared membranes at 4.5 bar for 1 h. After filtration the fouled membranes were kept in to the deionized water for 30 min. Then the pure water flux measured at 4.5 bar and 25°C by washed membrane to calculate the flux recovery ratio. The following equation was used to evaluate the flux recovery ratio:

$$FRR\% = \left(\frac{J_{w,2}}{J_{w,1}}\right) \times 100 \quad (5)$$

Where J_{w1} (L/m^2h) is the pure water flux of clean membrane and J_{w2} ($L.m^2h$) is the pure water flux of uncleaned membrane.

3. Results and discussion

3.1. Membrane Characterization

The chemical structure of modified membrane was characterized by FTIR as shown in Fig. 2. The peaks at 1089.26 and 1106 cm^{-1} are assigned to the cage structure of Si-O-Si groups which revealed the existence of POSS nanoparticles on the membrane surface. The peaks at 3000 and 3500 cm^{-1} are related to the presence of amine (–NH) and hydroxyl (–OH) functional groups. Peaks at 2958.25 and 2926.47 cm^{-1} are attributed to the stretching vibration of C-H bonds. Moreover, the peaks at 1665.05 cm^{-1} corresponded to the C=O stretching of the carboxyl groups [3, 6, 10].

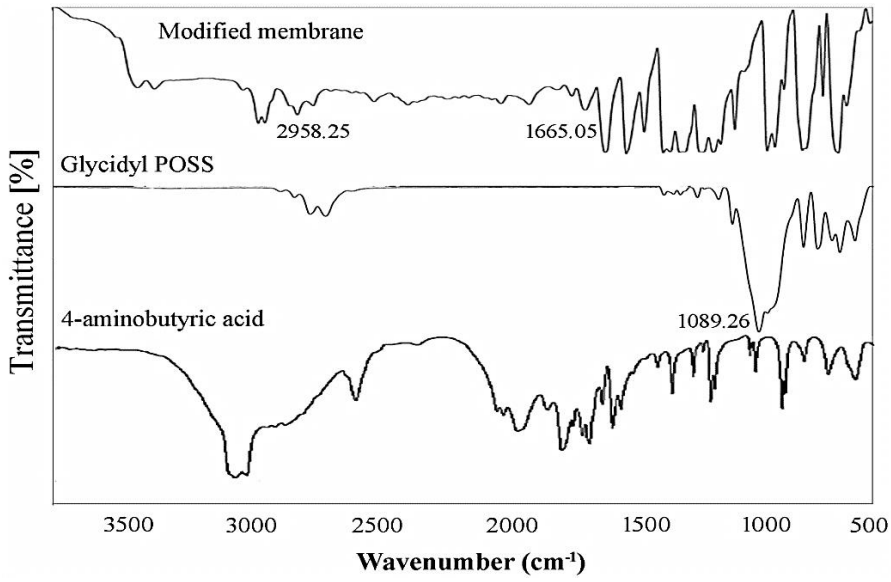

Fig. 2. FTIR spectra of 4-aminobutyric acid and glycidyl POSS and the modified membranes.

3.2. Membrane morphology

The cross-sectional and surface morphology of membranes are shown in Fig. 3. As seen, by increasing the concentration of POSS/4-aminobutyric acid on the top surface of membrane change the membrane morphology compare to the neat PES membrane. Moreover, the cross-sectional SEM images of the fabricated membranes

show an asymmetric and porous structure that is containing dense top layer and porous sub layer with finger like structure. By increasing the concentration of POSS/4-aminobutyric acid on the membrane surface increase the thickness of active layer that act as a barrier for ions transport. The uniform dispersion of POSS/4-aminobotyric acid is clear in the surface images of SEM. But in high concentration of POSS/4-aminobutyric acid occurred the accumulation of POSS particles. Moreover, by introducing POSS/4-aminobotyric acid increased porosity of the modified membranes in comparison to the virgin PES membrane because of the cage and porous structure of POSS. Fig. 4 presents EDX and mapping analysis for the modified membranes containing of COOH-POSS particles. The silicon (Si) element was observed from EDX analysis to confirm the existence of POSS/4-aminobutyric acid on the membrane surface. Moreover, EDX mapping indicated a uniform distribution of nanoparticles on the membrane surface. Fig. 5 shows the overall porosity for the prepared membranes. However, the membrane porosity declined for M2 and M3 compare to M1 that can be attributed to the pores filling phenomenon at the high concentration of COOH-POSS nanoparticles. The highest mean pore size was observed for M1, as illustrated in Fig. 6. The mean pore size of prepared membranes declined by increasing the concentration ratio of POSS to 4-aminobutyric acid compared to M1. As seen in SEM images, the pores of membrane are filled by the accumulation nanoparticles on the membrane surface that can be a reason to decrease the mean pure size of membrane at high concentration of nanoparticles [6, 10].

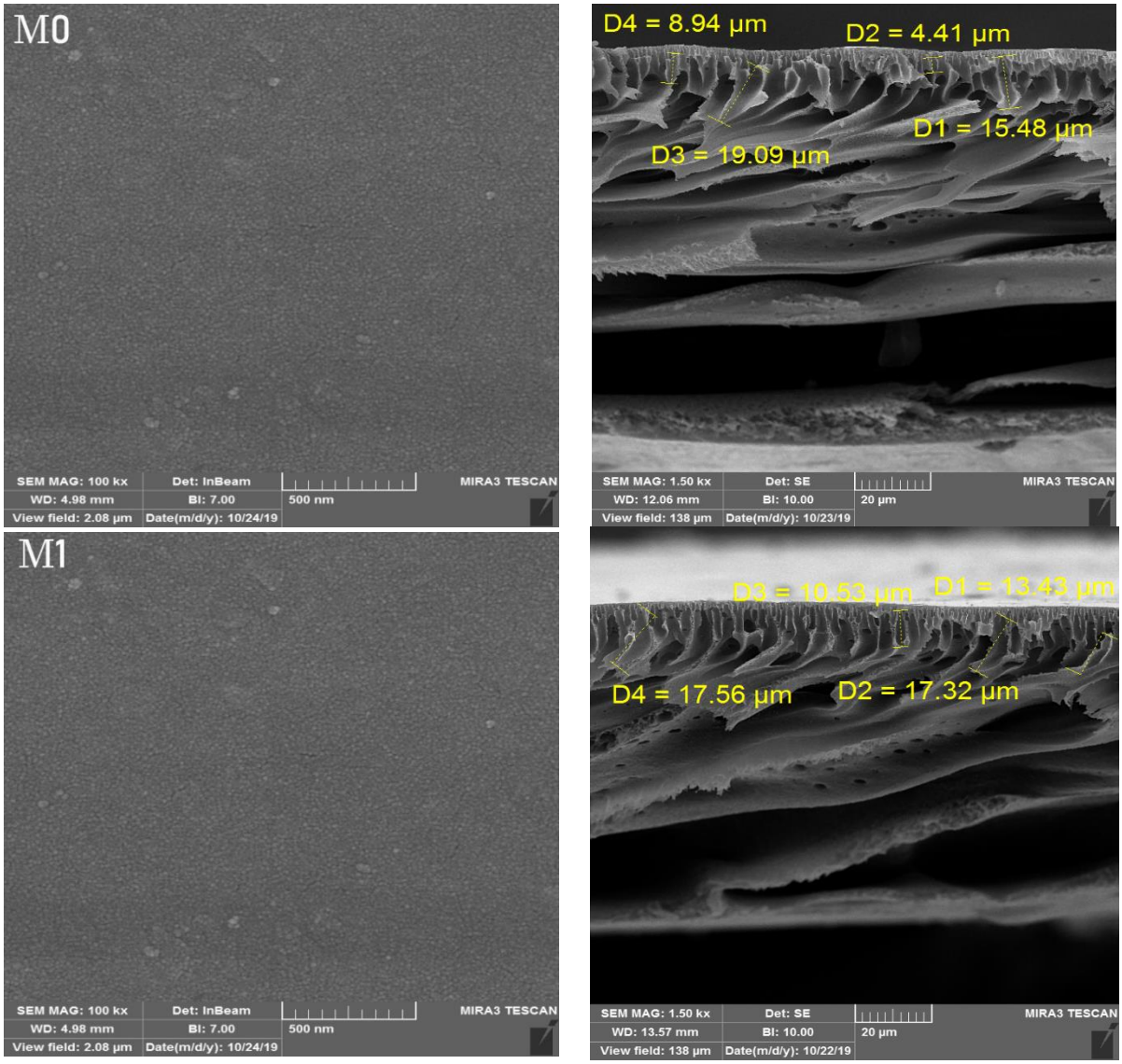

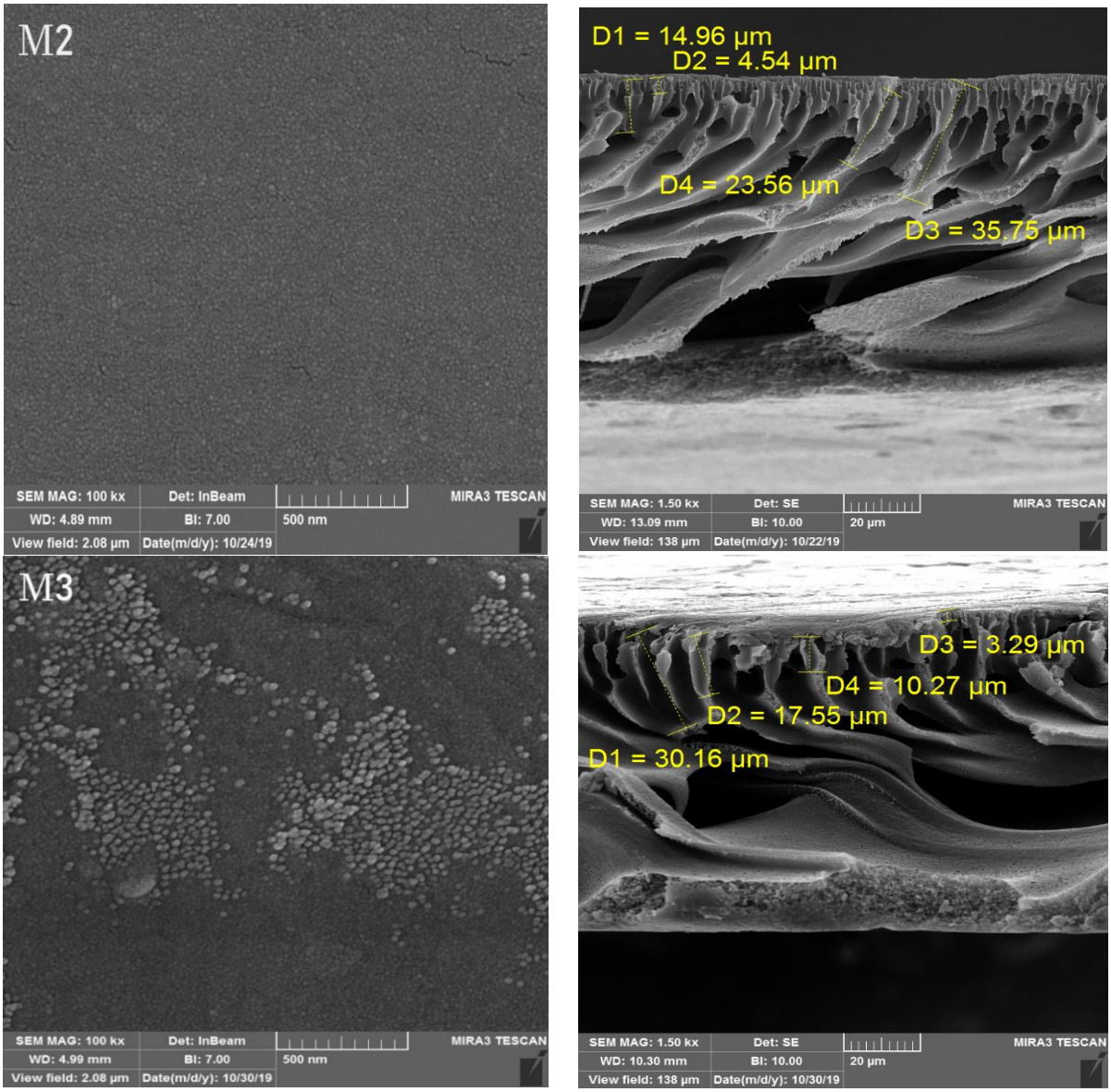

Fig. 3. SEM images of pure PES and modified membranes.

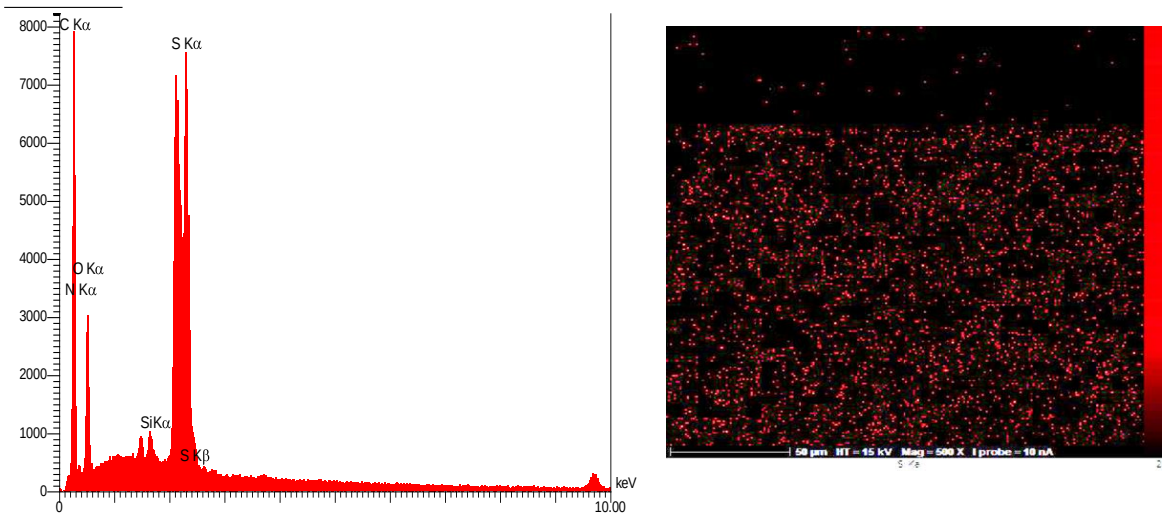

Fig. 4. EDX elemental analysis and dot mapping distribution of Si element for modified membrane (M3).

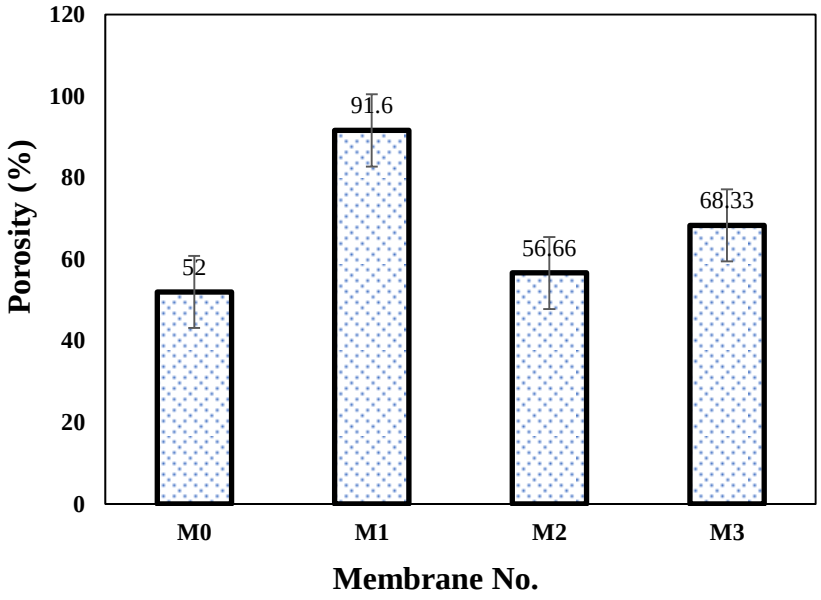

Fig. 5. The porosity of bare PES and modified membranes.

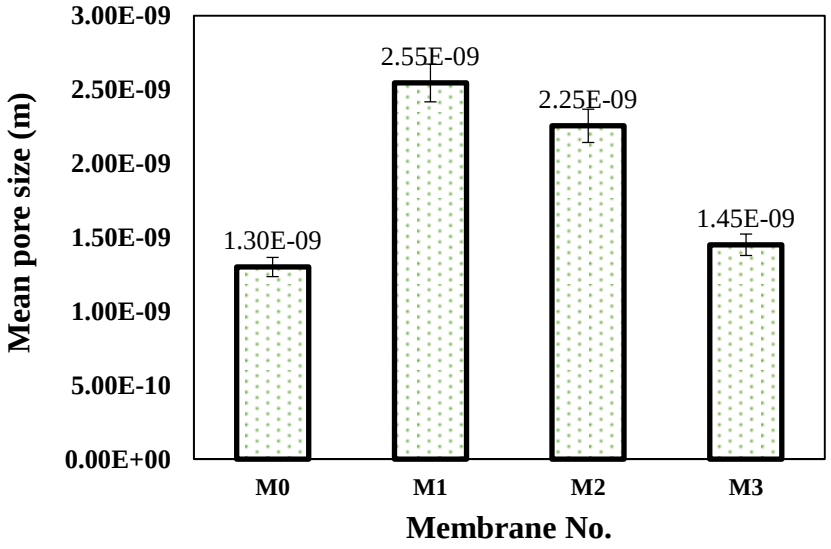

Fig. 6. Mean pore size of bare PES and modified membranes.

The surface morphology of the produced membrane was appraised by three-dimensional surface images by SPM software (version 6.4, Femtoscan). The results of 3D surface images were investigated in terms of roughness average (R_a), root mean square roughness (R_q), and maximum height of roughness (R_{max}) as given in Fig. 7 and Table 1. The results revealed that surface of neat PES membrane is rougher than the surface of PES/COOH-POSS membranes and the R_a declined from 5 nm for M0 to 3.9 nm for M3. This trend is due to the placement of COOH-POSS on the membrane surface with uniformly distribution which fills the valleys on the surface of membrane and decrease the surface roughness [32, 33].

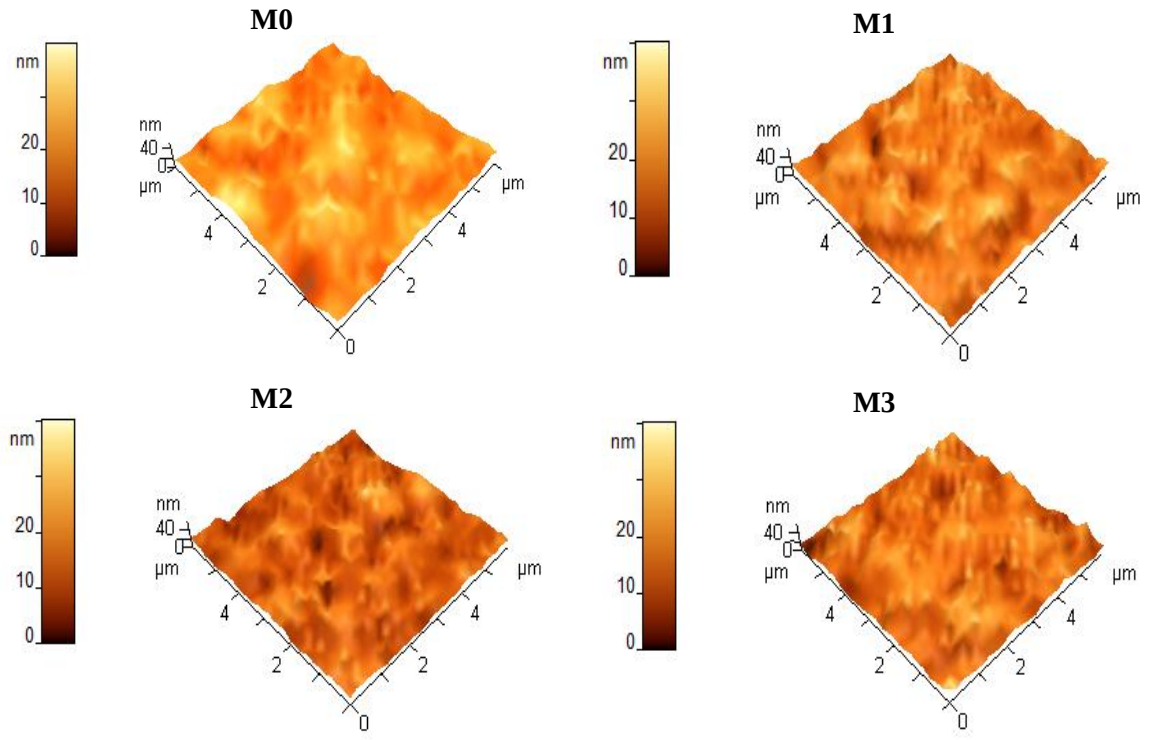

Fig. 7. 3D surface images for the fabricated membranes.

Table 1. Detail of surface roughness parameter for the fabricated membranes.

Sample	R_a (nm)	R_{max} (nm)	R_q (nm)
M0	5.086	22.16	6.142
M1	4.309	20.51	5.334
M2	4.052	20.05	4.968
M3	3.905	19.83	4.843

3.2. Water content and contact angle

The water content and contact angle of the fabricated membranes are appropriate criterion for measuring the hydrophilicity of membrane. As seen in Table 2, the water contact angle declined from 62° for the bare PES to 40° for M3 which introduce a more hydrophilic surface for the modified membrane by introducing COOH-POSS on the membrane surface. This may be assigned to the presence of carboxyl (–COOH), hydroxyl (–OH) and amine (–NH) groups on the membrane surface. Also by increasing the amount of nanoparticles on the membrane surface, the water content increased from 68 to 77.35% that can be explained by the cage and porous structure of POSS [21, 34, 35].

Table 2. Water content and contact angle of the bare PES and modified membranes.

Sample	Contact angle (°)	Water content (%)
M0	62	68
M1	43	75.86
M2	50	73.11
M3	40	77.35

4. Fabricated membrane performance

4.1. Pure water flux

Fig. 7 demonstrate the result of pure water flux. The pure water flux decreased from 12.08 (L/m^2h) for the neat PES membrane to 5.6 for M3. This phenomenon can be described by the agglomeration of nanoparticles on the surface of membrane which blocks the pores and decrease PWF of prepared membrane. Also as seen in SEM images the thickness of top layer raised by accumulation of nanoparticles at higher concentration that caused to decrease the pure water flux of modified membranes [36] .

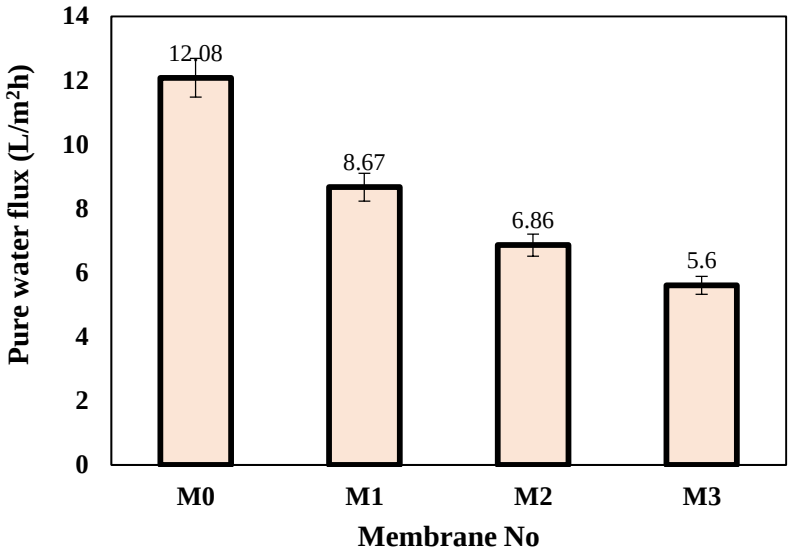

Fig. 7. Pure water flux of the prepared membranes.

4.2. Salt and heavy metal rejection

The performance of the fabricated membranes were evaluated via the rate of flux and rejection of Na_2SO_4 and heavy metals ($Pb(NO_3)_2$, $CrSO_4$ and $Cu(NO_3)_2$). As presented in Fig. 8 the rejection of Na_2SO_4 increased from 40.76% for the pure PES membrane to 62% for M3 at 1.5 wt.% COOH-POSS. Donnan exclusion is the most effective mechanisms on salt rejection [36]. Also the formation of dense structure on the membrane surface is another element that increases salt rejection (as seen the SEM image of M3) [37, 38] .

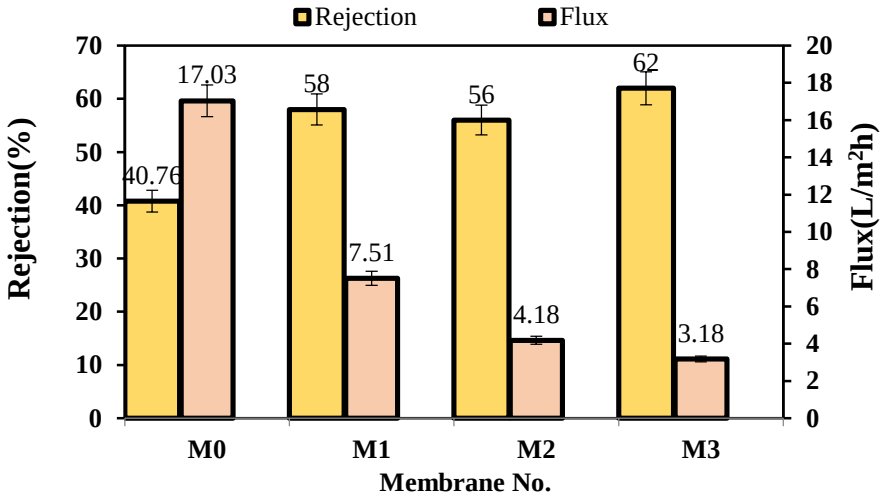

Fig. 8. The salt rejection of membranes for Na_2SO_4 aqueous solution.

Fig. 9 demonstrate the rejection of $CrSO_4$ for the prepared membranes at different concentration of COOH-POSS. The obtained results show the improvement of $CrSO_4$ rejection from 45% for the bare PES membrane to 80% for M3 at 1.5 wt.% COOH-POSS . Adsorption mechanism is considered as a main factor to improve the $CrSO_4$ ejection. Also the repulsion of SO_4^{2-} ions is due to the presence of negative charges functional groups on the membrane surface. The highest $Cu(NO_3)_2$ rejection was obtained 80% for M1 at 0.5 wt.% of COOH-POSS as illustrated in Fig. 10. Enhancement of $Cu(NO_3)_2$ rejection is explained by the adsorption sites of POSS structure and the presence of negative charges on the surface of membranes. Nevertheless, $Cu(NO_3)_2$ rejection decline at high concentration of COOH-POSS is thanks to the agglomeration of nanoparticles, pore blocking and decreasing active sites. Fig. 11 reveals the obtained data from $Pb(NO_3)_2$ rejection for the neat PES and modified membranes at diverse content of COOH-POSS.

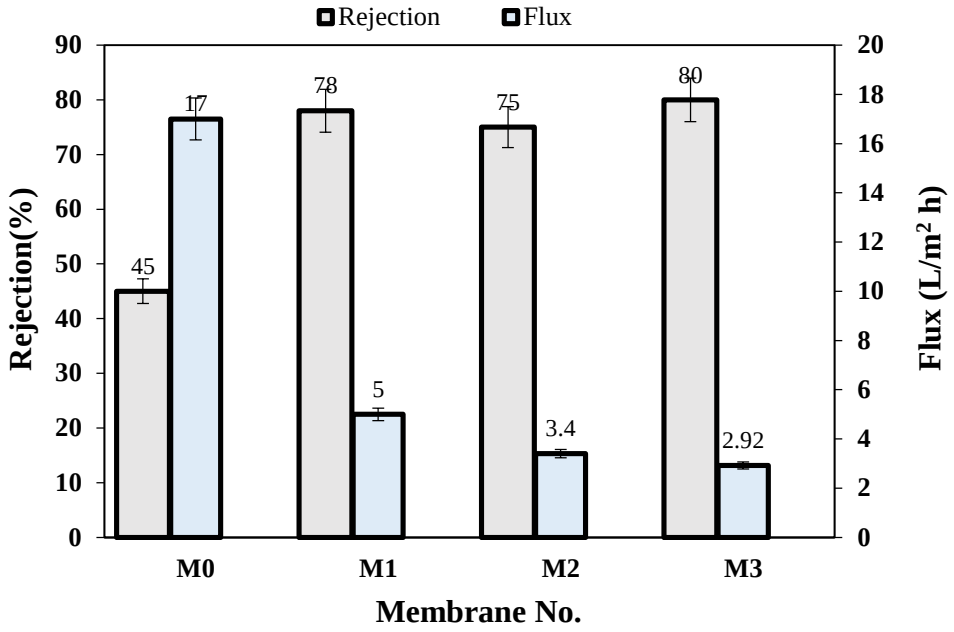

Fig. 9. The $CrSO_4$ rejection of bare PES and modified membranes.

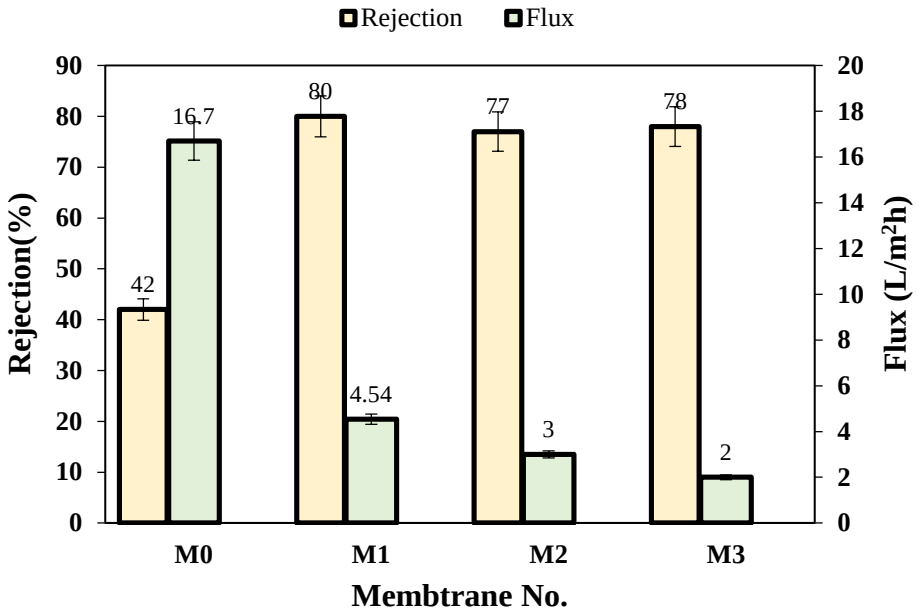

Fig. 10. The heavy metal rejection of membranes for $Cu(NO_3)_2$ aqueous solution.

The $Pb(NO_3)_2$ rejection was raised from 31% for the pristine PES membrane to 83% for M1 at 0.5 wt.% nanoparticles. The significant improvement of $Pb(NO_3)_2$ rejection is attributed to the cage structure of POSS that create active sites for adsorption of Pb^{2+} ions. Moreover, negative charges on the membrane surface lead to repulse NO_3^- ions. However by increase of POSS: 4-aminobutyric acid ratio, the $Pb(NO_3)_2$ rejection reduces in the comparison to M1 membrane. The decrease in $Pb(NO_3)_2$ rejection at high content of COOH-POSS may be due to nanoparticles accumulation on the membrane surface. It was found that COOH-POSS has high capacity in heavy metal separation.

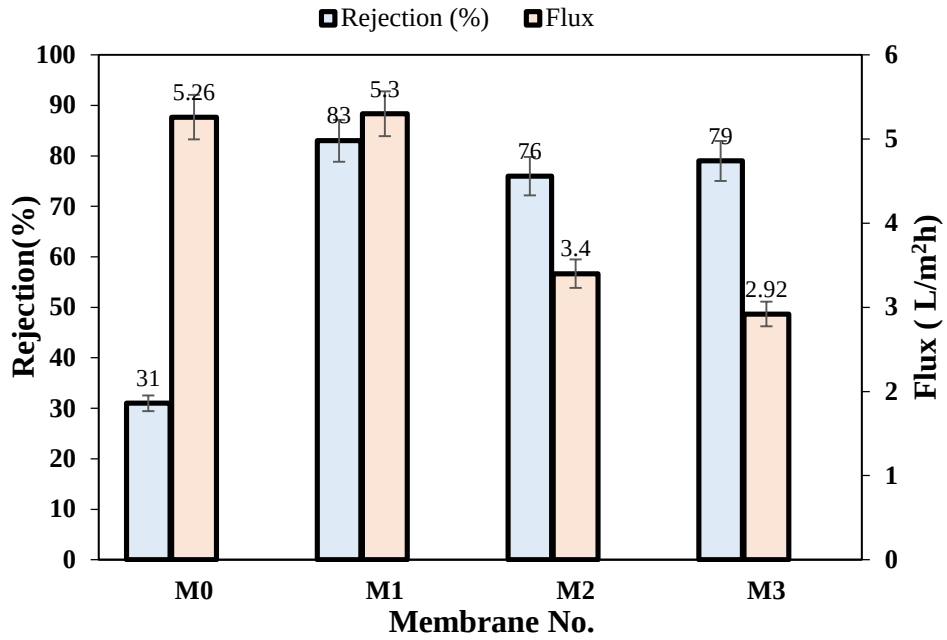

Fig. 11. The heavy metal rejection of membranes for $Pb(NO_3)_2$ aqueous solution.

4.3. Antifouling performance

Membrane fouling is one of the major problem in nanofiltration membranes which is affected by the surface roughness, surface charge, surface functional groups and wettability [39]. Fouling decreases the permeation flux, selectivity and the life time of membrane. Antifouling performance of resulted membrane was investigated by the flux recovery ratio (FRR) as displayed in Fig.12. The results show the highest FRR% (63.32%) for M2 membrane. It was found from FRR% that modified membranes have better antifouling performance than unmodified membrane but as seen the FRR% of M1 has declined in comparison to bare PES membrane. This phenomenon can be explained by COOH-POSS accumulation on the membrane surface (see surface images of SEM). Moreover, the obtained results from FRR% and 3D surface images data indicate that the decrease of membrane surface roughness leads to lower fouling [40,41,42, 43].

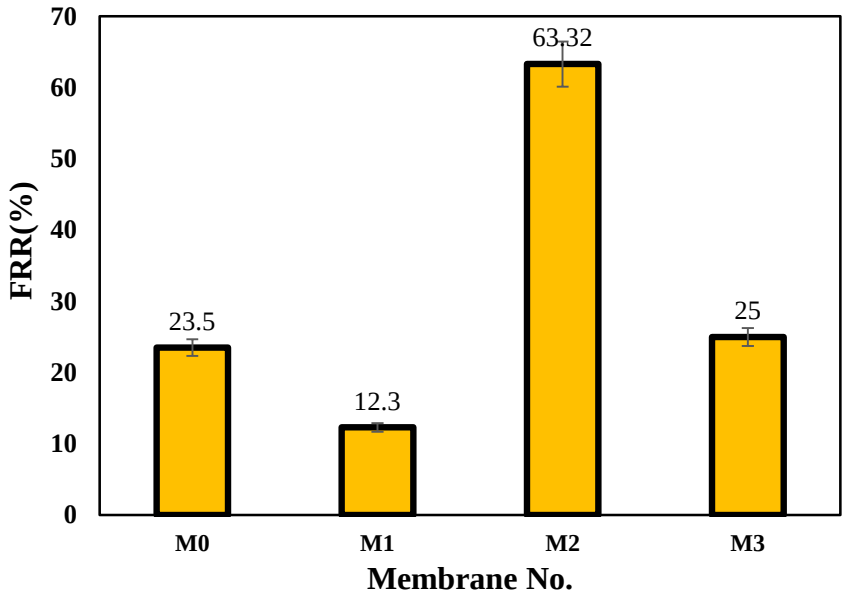

Fig. 12. The flux recovery ratio (FRR%) of bare PES and modified membranes.

5. Conclusion

The surface modification of NF membranes was performed to achieve high separation performance. The membranes water content, content angle, porosity, mean pore size, pure water flux, Na_2SO_4 rejection and heavy metal rejection ($Pb(NO_3)_2$, $CrSO_4$ and $Cu(NO_3)_2$) of membranes were studied. Membrane hydrophilicity and negative charges on the membrane surface increased due to the present of carboxyl, hydroxyl and amine groups into the COOH-POSS structure. It was found that salt rejection was affected by Donnan exclusion. Moreover, adsorption mechanism was the main factor to improve the heavy metal rejection of the modified membranes. Also FRR% increased from 23.5 % for the virgin PES membrane to 63.32% for the modified membrane (M2). SEM images clearly reveal a dense top layer and finger-like structure. However, the pure water flux revealed the decline trend. But among prepared membranes, M3 at 1.5 wt.% COOH-POSS concentration showed the best $CrSO_4$ rejection (80%) and Na_2SO_4 rejection (62%). Moreover, M1 at 0.5 wt.% of COO-POSS showed the $Cu(NO_3)_2$ and $Pb(NO_3)_2$ rejection 80% and 83%, respectively.

Conflicts of Interest

The author declares no conflict of interest.

Author information

*Corresponding Author: Abdolreza Moghadassi, Samaneh Bandehali
E-mail address: a-moghadassi@araku.ac.ir, s-bandehali@phd.araku.ac.ir

ORCID
Abdolreza Moghadassi: 0000-0003-0733-4540.

References

[1] Z. Tan, S. Chen, X. Peng, L. Zhang, C. Gao, Polyamide membranes with nanoscale Turing structures for water purification, Sci., 360 (2018) 518-521. https://doi.org/10.1126/science.aar6308.
[2] M. Tao, L. Xue, F. Liu, L. Jiang, An intelligent superwetting PVDF membrane showing switchable transport performance for oil/water separation, Adv. Mater. , 26 (2014) 2943-2948. https://doi.org/10.1002/adma.201305112.
[3] S. Bandehali, F. Parvizian, A. Moghadassi, S.M. Hosseini, High water permeable PEI nanofiltration membrane modified by L-cysteine functionalized POSS nanoparticles with promoted antifouling/separation performance, Sep. Purif. Technol., 237 (2019) 116361. https://doi.org/ j.seppur.2019.116361
[4] S.M. Hosseini, M. Afshari, A.R. Fazlali, S. Koudzari Farahani, S. Bandehali, B. Van der Bruggen, E. Bagheripour, Mixed matrix PES-based nanofiltration membrane decorated by (Fe_3O_4–polyvinylpyrrolidone) composite nanoparticles with intensified antifouling and separation characteristics, Chem. Eng. Res. Des., 147 (2019) 390-398. https://doi.org/10.1016/j.cherd.2019.05.025.
[5] L.-C. Juang, D.-H. Tseng, H.-Y. Lin, Membrane processes for water reuse from the effluent of industrial park wastewater treatment plant: A study on flux and fouling of membrane, Desalination, 202 (2007) 302-309. https://doi.org/10.1016/j.desal.2005.12.068.
[6] S. Bandehali, A. Moghadassi, F. Parvizian, Y. Zhang, S. Mohsen Hosseini, J. Shen, New mixed matrix PEI nanofiltration membrane decorated by glycidyl-POSS functionalized graphene oxide nanoplates with enhanced separation and antifouling behaviour: heavy metal ions removal, Sep. Purif. Technol., (2020) 116745. https://doi.org/10.1016/j.seppur.2020.116745.
[7] A. Bhattacharya, B. Misra, Grafting: A versatile means to modify polymers: techniques, factors and applications, Prog. Polym. Sci., 29 (2004) 767-814. https://doi.org/j.progpolymsci.2004.05.002.
[8] S. Bandehali, F. Parvizian, A.R. Moghadassi, S.M. Hosseini, Copper and lead ions removal from water by new PEI based NF membrane modified by functionalized POSS nanoparticles, J. Polym. Res., 26 (2019) 211-219. https://doi.org/10.1007/s10965-019-1865-7.
[9] Bandehali, Samaneh, Fahime Parvizian, Abdolreza Moghadassi, and Sayed Mohsen Hosseini. "Nanomaterials for the efficient abatement of wastewater contaminants by means of reverse osmosis and nanofiltration." In Nanomaterials for the Detection and Removal of Wastewater Pollutants, pp. 111-144. Elsevier, 2020. https://doi.org/10.1016/B978-0-12-818489-9.00005-0.
[10] F. Parvizian, F. Ansari, S. Bandehali, Oleic acid-functionalized TiO_2 nanoparticles for fabrication of PES-based nanofiltration membranes, Chem. Eng. Res. Des., 156 (2020) 433-441. https://doi.org/10.1016/j.cherd.2020.02.019.
[11] M. Maarefian, S. Bandehali, S. Azami, H. Sanaeepur, A. Moghadassi, Hydrogen recovery from ammonia purge gas by a membrane separator: A simulation study, Int. J. Energy Chem., 43 (2019) 8217-8229. https://doi.org/10.1002/er.4819.
[12] D.J. Miller, D.R. Dreyer, C.W. Bielawski, D.R. Paul, B.D. Freeman, Surface modification of water purification membranes, Angew. Chem., Int. Ed., 56 (2017) 4662-4711, https://doi.org/10.1002/anie.201601509.

[13] S. Bandehali, A. Moghadassi, F. Parvizian, J. Shen, S. Hosseini, Glycidyl POSS-functionalized ZnO nanoparticles incorporated polyether-imide based nanofiltration membranes for heavy metal ions removal from water, Korean J. Chem. Eng., 37 (2020) 263-273. https://doi.org/s11814-019-0441-5.
[14] Seidypoor, Amin, Ezatollah Joudaki, Sayed Mohsen Hosseini, and Samaneh Bandehali, Double-layer electrodialysis cation exchange membrane by introducing chitosan/TiO_2 thin-film nanocomposite on PVC-based substrate for Cu removal from water, Ionics., 28, no. 6 (2022): 3037-3048. https://doi.org/s11581-022-04518-2.
[15] Bandehali, Samaneh, Fahime Parvizian, Sayed Mohsen Hosseini, Takeshi Matsuura, Enrico Drioli, Jiangnan Shen, Abdolreza Moghadassi, and Adeyemi S. Adeleye,Planning of smart gating membranes for water treatment, Chemosphere., 283 (2021): 131207. https://doi.org/10.1016/j.chemosphere.2021.131207.
[16] S. Bandehali, A. Kargari, A. Moghadassi, H. Sanaeepur, D. Ghanbari, Acrylonitrile–butadiene–styrene/poly (vinyl acetate)/nanosilica mixed matrix membrane for He/CH_4 separation, Asia-Pac J. Chem. Eng., 9 (2014) 638-644. https://doi.org/10.1002/apj.1792.
[17] S. Bandehali, A. Moghadassi, F. Parvizian, S.M. Hosseini, T. Matsuura, E. Joudaki, Advances in high carbon dioxide separation performance of poly (ethylene oxide)-based membranes, J. Energy Chem., 46 (2020) 30-52. https://doi.org/10.1016/j.jechem.2019.10.019.
[18] S. Bandehali, F. Parvizian, A.R. Moghadassi, S.M. Hosseini, J.N. Shen, Fabrication of thin film-PEI nanofiltration membrane with promoted separation performances: Cr, Pb and Cu ions removal from water, J. Polym. Res., 27 (2020) 94. https://doi.org/10.1007/s10965-020-02056-x.
[19] C. Xiong, Z. Huang, Z. Ouyang, M. Tang, X. Lin, Z. Zhang, Improvement of the separation and antibiological fouling performance using layer-by-layer self-assembled nanofiltration membranes, J. Coat Technol. Res., (2020) 1-16. https://doi.org/10.1007/s11998-019-00298-z.
[20] X. Huang, Y. Chen, X. Feng, X. Hu, Y. Zhang, L. Liu, Incorporation of oleic acid-modified Ag@ZnO core-shell nanoparticles into thin film composite membranes for enhanced antifouling and antibacterial properties, J. Membr. Sci., (2020) 117956. https://doi.org/10.1016/j.memsci.2020.117956.
[21] G. Li, B. Liu, L. Bai, Z. Shi, X. Tang, J. Wang, H. Liang, Y. Zhang, B. Van der Bruggen, Improving the performance of loose nanofiltration membranes by poly-dopamine/zwitterionic polymer coating with hydroxyl radical activation, Sep. Purif. Technol., 238 (2020) 116412. https://doi.org/10.1016/j.seppur.2019.116412.
[22] J. Nan Shen, C. chao Yu, H. min Ruan, C. jie Gao, B. Van der Bruggen, Preparation and characterization of thin-film nanocomposite membranes embedded with poly (methyl methacrylate) hydrophobic modified multiwalled carbon nanotubes by interfacial polymerization, J. Membr. Sci., 442 (2013) 18-26. https://doi.org/10.1016/j.memsci.2013.04.018.
[23] V. Vatanpour, S.J.M.C. Khorshidi, Physics, Surface modification of polyvinylidene fluoride membranes with ZIF-8 nanoparticles layer using interfacial method for BSA separation and dye removal, Mater. Chem. Phys., 241 (2020) 122400. https://doi.org/10.1016/j.matchemphys.2019.122400.
[24] A. Stepanov, Polymer Composites with Functionalized Nanoparticles, in, Elsevier Amsterdam, The Netherlands, 2019. https://doi.org/10.1016/B978-0-12-814064-2.00010-X.
[25] N. Koutahzadeh, M.R. Esfahani, F. Bailey, A. Taylor, A.R. Esfahani, Enhanced performance of polyhedral oligomeric silsesquioxanes/polysulfone nanocomposite membrane with improved permeability and antifouling properties for water treatment, J. Environ. Chem. Eng., 6 (2018) 5683-5692. https://doi.org/10.1016/j.jece.2018.08.049.
[26] S. Dong, J. Feng, M. Fan, Y. Pi, L. Hu, X. Han, M. Liu, J. Sun, J. Sun, Recent developments in heterogeneous photocatalytic water treatment using visible light-responsive photocatalysts: A review, Rsc Adv., 5 (2015) 14610-14630. https://doi.org/10.1039/C4RA13734E.
[27] X. You, T. Ma, Y. Su, H. Wu, M. Wu, H. Cai, G. Sun, Z. Jiang, Enhancing the permeation flux and antifouling performance of polyamide nanofiltration membrane by incorporation of PEG-POSS nanoparticles, J. Membr. Sci., 540 (2017) 454-463. https://doi.org/10.1016/j.memsci.2017.06.084.
[28] Y. He, Y.P. Tang, D. Ma, T.-S. Chung, UiO-66 incorporated thin-film nanocomposite membranes for efficient selenium and arsenic removal, J. Membr. Sci., 541 (2017) 262-270. https://doi.org/10.1016/j.memsci.2017.06.061.
[29] S.-m. Lee, J.-y. Jung, Y.-c. Chung, Novel method for enhancing permeate flux of submerged membrane system in two-phase anaerobic reactor, Water Res., 35 (2001) 471-477. https://doi.org/10.1016/S0043-1354(00)00255-4.
[30] D. Rana, T. Matsuura, Surface modifications for antifouling membranes, Chem. Rev., 110 (2010) 2448-2471, https://doi.org/10.1021/cr800208y.
[31] S. Bandehali, A. Moghadassi, F. Parvizian, S. Hosseini, A new type of [PEI-glycidyl POSS] nanofiltration membrane with enhanced separation and antifouling performance, Korean J. Chem. Eng., 36 (2019) 1657-1668. https://doi.org/10.1007/s11814-019-0359-y.
[32] F. Zareei, S.M. Hosseini, A new type of polyethersulfone based composite nanofiltration membrane decorated by cobalt ferrite-copper oxide nanoparticles with enhanced performance and antifouling property, Sep. Purif. Technol., 226 (2019) 48-58. https://doi.org/10.1016/j.seppur.2019.05.077.

[33] S. Ansari, E. Bagheripour, A. Moghadassi, S.M. Hosseini, Fabrication of mixed matrix poly (phenylene ether-ether sulfone)-based nanofiltration membrane modified by Fe_3O_4 nanoparticles for water desalination, J. Polym. Eng., 37 (2017) 61-67. https://doi.org/10.1515/polyeng-2015-0392.
[34] Y. Yuan, X. Gao, Y. Wei, X. Wang, J. Wang, Y. Zhang, C. Gao, Enhanced desalination performance of carboxyl functionalized graphene oxide nanofiltration membranes, Desalination, 405 (2017) 29-39. https://doi.org/10.1016/j.desal.2016.11.024.
[35] S. Abdikheibari, W. Lei, L.F. Dumée, N. Milne, K. Baskaran, Thin film nanocomposite nanofiltration membranes from amine functionalized-boron nitride/polypiperazine amide with enhanced flux and fouling resistance, J. Mater. Chem. A, 6 (2018) 12066-12081. https://doi.org/10.1039/C8TA03446J.
[36] F. Zareei, S.M. Hosseini, A new type of polyethersulfone based composite nanofiltration membrane decorated by cobalt ferrite-copper oxide nanoparticles with enhanced performance and antifouling property, Sep. Purif. Technol., 226 (2019) 48-58. https://doi.org/10.1016/j.seppur.2019.05.077.
[37] J. Zhu, M. Tian, Y. Zhang, H. Zhang, J. Liu, Fabrication of a novel "loose" nanofiltration membrane by facile blending with Chitosan–Montmorillonite nanosheets for dyes purification, J. Chem. Eng., 265 (2015) 184-193. https://doi.org/10.1016/j.cej.2014.12.054.
[38] X. Cheng, C. Lai, X. Zhu, S. Shao, J. Xu, F. Zhang, J. Song, D. Wu, H. Liang, X. Luo, Tailored ultra-low pressure nanofiltration membranes for advanced drinking water treatment, Desalination,. 548 (2023) 116264. https://doi.org/10.1016/j.desal.2022.116264.
[39] S. Yuan, J. Li, J. Zhu, A. Volodine, J. Li, G. Zhang, P. Van Puyvelde, B. Van der Bruggen, Hydrophilic nanofiltration membranes with reduced humic acid fouling fabricated from copolymers designed by introducing carboxyl groups in the pendant benzene ring, J. Membr. Sci, 563 (2018) 655-663. https://doi.org/10.1016/j.memsci.2018.06.038.
[40] Y. Li, S. Huang, S. Zhou, A.G. Fane, Y. Zhang, S. Zhao, Enhancing water permeability and fouling resistance of polyvinylidene fluoride membranes with carboxylated nanodiamonds, J. Membr. Sci, 556 (2018) 154-163. https://doi.org/10.1016/j.memsci.2018.04.004.
[41] A. Moghadassi, S. Ghohyei, S. Bandehali, M. Habibi, M. Eskandari, Cuprous oxide (Cu_2O) nanoparticles in nanofiltration membrane with enhanced separation performance and anti-fouling properties, Korean J. Chem. Eng, 40 (2023) 630–641. https://doi.org/10.1007/s11814-022-1249-2.
[42] A. Seidypoor, S. Bandehali, M. Ebrahimi, H. Solhi, E. Joudaki, S. M. Hosseini, Fabrication of layer-by-layer ion exchange membrane by applying PDA-POSS nanocomposite onto heterogeneous cationic substrate for water treatment, Colloid Nanosci. J., 1 (2023) 51-61. https://doi.org/10.52547/CNJ.1.1.51.
[43] A. Seidypoor, E. Joudaki, S. Bandehali, S. Solhi, S. M. Hosseini, A novel electrodialysis membrane, modified by polydopamine and carbon nanofibers, removes toxic heavy metal ions from wastewaters. Iran. J. Toxicol., 17 (2023) 33-42. https://doi.org/10.52547/ijt.17.1.4.